Tissue-specific requirements for FGF8 during early inner ear development

Elena Domínguez-Frutos[1], Victor Vendrell[2], Yolanda Alvarez[2], Laura Cecilia Zelarayan[2], Iris López-Hernández[1], Marian Ros[3] and Thomas Schimmang[1,2]

[1]Instituto de Biología y Genética Molecular, Universidad de Valladolid y Consejo Superior de Investigaciones Científicas, Centro de Investigación Biomédica en Red sobre Enfermedades Neurodegenerativas (CIBERNED), C/Sanz y Forés s/n, E-47003 Valladolid, Spain [2]Center for Molecular Neurobiology, University of Hamburg, Falkenried 94, D-20251 Hamburg, Germany, [3]Instituto de Biomedicina y Biotecnología de Cantabria, IBBTEC (CSIC-UC-IDICAN) C/ Herera Oria s/n, E-39011 Santander, Spain

Corresponding author: Dr. Thomas Schimmang

IBGM

C/Sanz y Forés s/n

47003 Valladolid, Spain

Tel.: +34983184818

Fax: +34983184800

Email: schimman@ibgm.uva.es

Running title: Roles of FGF8 during otic induction

Key words: Fibroblast growth factor, otic vesicle, otic placode, mouse, chicken

Abstract

Several members of the FGF gene family have been shown to intervene from various tissue sources to direct otic placode induction and otic vesicle formation. In this study we define the roles of FGF8, found in different expression domains during this process, in mice and chickens. By conditional inactivation of *Fgf8* in distinct tissue compartments we demonstrate that *Fgf8* is required in the mesoderm and endoderm during early inner ear development. In the chicken embryo, overexpression of *Fgf8* from various tissue sources during otic specification leads to a loss of otic tissue. In contrast ectopic overexpression of *Fgf10*, a major player during murine otic induction, does not influence otic vesicle formation in chicken embryos but results in the formation of ectopic structures with a non-otic character. This study underlines the crucial role of a defined *Fgf8* expression pattern controlling inner ear formation in vertebrates.

Introduction

Early inner ear development in vertebrates is initiated by signals derived from the endoderm and mesoderm underneath the preplacodal ectoderm. In a second phase a neural signal from the developing hindbrain completes the induction process and ends with the specification of part of the preplacodal ectoderm to form the otic placode The otic placode will then invaginate to form the otic vesicle and differentiate to the mature inner ear (Bailey and Streit, 2006; Groves, 2005; Groves and Bronner-Fraser, 2000).

Various members of the Fibroblast growth factor (FGF) gene family have been shown to control different aspects of early inner ear development (Schimmang, 2007). During both mouse and chicken inner ear development FGF8 has been postulated as the first signal initiating otic induction (Ladher et al., 2005). Loss-of-function experiments based on the electroporation of siRNA directed against *Fgf8* in the chicken embryo at HH4 leads to loss of placodal tissue. The source of *Fgf8* expression has been localized to the endoderm where it is expressed from HH6 (Hamburger and Hamilton, 1992) onwards. The function of *Fgf8* apparently consists in inducing *Fgf19* expression in the overlying mesoderm (Ladher et al., 2005). *Fgf3* expression in the mesoderm is simultaneously observed to *Fgf19* expression but the requirement of *Fgf8* for *Fgf3* expression has not been examined (Kil et al., 2005). A similar sequence of events also appears to operate during the initiation of otic induction in mouse. *Fgf8* initiates its expression at E7 in the mesoderm but is additionally detected in the endoderm and preplacodal ectoderm at E8 (Crossley and Martin, 1995; Ladher et al., 2005; Zelarayan et al., 2007). Loss-of-function experiments in mice have shown that *Fgf8* is redundantly required together with *Fgf3* for formation of the otic placode and vesicle (Ladher et al., 2005; Zelarayan et al., 2007). Both Fgfs also are required for normal levels of *Fgf10*

expression in the mesoderm during otic induction (Ladher et al., 2005). During E8 *Fgf3* is initially observed in the neural tube and preplacodal ectoderm (Wright and Mansour, 2003) and has only been later described in the pharyngeal endoderm shortly before placode invagination (Mahmood et al., 1996; McKay et al., 1996). Likewise in the chick, the initial expression of *Fgf3* in the mesoderm is accompanied by additional expression domains in the pharyngeal endoderm and neural tube when the otic placode has been specified to form in the preplacodal ectoderm (Mahmood et al., 1995). The relevance of these expression domains has been examined by siRNA-mediated knockdown of *Fgf3* (Freter et al., 2008; Zelarayan et al., 2007). In these experiments *Fgf3* has been shown to be required for otic placode induction (Freter et al., 2008) and the transition of the otic placode to the otic vesicle (Zelarayan et al., 2007). During placode formation and invagination *Fgf8* is maintained in the pharyngeal endoderm in chicken and mice (Adamska et al., 2001; Hidalgo-Sanchez et al., 2000; Stolte et al., 2002). In chicken, FGF8 beads implanted into the mesoderm next to the otic placode at HH10 have been shown to increase otic marker gene expression and the size of the normal otic vesicle (Adamska et al., 2001). Finally in both chicken and mice *Fgf10* is expressed in the otic placode itself (Alsina et al., 2004; Alvarez et al., 2003; Karabagli et al., 2002; Ohuchi et al., 1997; Pirvola et al., 2000; Wright and Mansour, 2003). The relevance of *Fgf10* expression for otic placode and vesicle formation at this stage has so far not been addressed.

In the present study we analyse the significance of the distinct *Fgf8* expression domains during early inner ear development in chicken and mice. Inactivation of *Fgf8* expression in the mesoderm in a homozygous *Fgf3* null background during murine otic induction leads to a severe loss or absence of otic tissue. Similar experiments targeting the endodermal domain of *Fgf8* expression also affects otic vesicle formation but in a

less severe manner. In the chicken embryo overexpression of *Fgf8* during otic placode specification and formation, when endogenous *Fgf8* is expressed in pharyngeal endoderm, leads to a reduced size of the otic vesicle. On the other hand *Fgf10*, endogenously present in the otic placode, does not affect otic vesicle formation upon its misexpression in periotic areas but leads to the formation of ectopic tissue with a non-otic character. These data confirm the requirement for a defined expression pattern of members of the FGF gene family in specific tissue domains during different phases of early inner ear development.

Results

Global loss of Fgf3 and specific inactivation of Fgf8 in the mesoderm during otic induction results in a severe reduction of otic tissue

Fgf3 and *Fgf8* have been shown to be redundantly required during otic induction in mice (Ladher et al., 2005; Zelarayan et al., 2007). However, the exact tissue source of *Fgf8* expression required during this process has not been defined. During otic induction between E7 to E8.5, *Fgf8* expression is initially observed in the mesoderm underneath the preplacodal ectoderm (Fig. 1A, Ladher et al. 2005). To determine the tissue-specific requirements for *Fgf8* during otic induction a conditional approach using Cre-LoxP-mediated disruption of *Fgf8* was used. We examined the relevance of *Fgf8* expression within the mesoderm by using a transgenic mouse line where Cre recombinase expression is controlled by the *MesP1* promoter, that has previously been shown to activate floxed reporter alleles, including $Fgf8^{GFP}$, specifically in the mesoderm during E8 (Park et al., 2006; Saga et al., 1999). We confirmed Cre activity in the mesoderm

and its absence in the endoderm using ROSA26 reporter mice at E7.75 (Supplementary Fig. 1A) To study the requirement for *Fgf8* expression in this domain during otic placode induction, we analysed the effects of conditional inactivation of *Fgf8* induced by Cre driven by the *MesP1* locus in a *Fgf3* null mutant background at the otic vesicle stage. We therefore crossed *Fgf3*$^{+/-}$/*Fgf8*$^{d2,3/+}$;*MesP1*$^{Cre/+}$ animals with *Fgf3*$^{-/-}$/*Fgf8*$^{flox/flox}$ mice. Upon external examination of *Fgf3*$^{-/-}$/*Fgf8*$^{flox/d2,3}$; *MesP1*$^{Cre/+}$ mutant embryos at E9 we failed to detect an otic vesicle. Histological analysis of these mutants (n=4) confirmed that otic vesicle formation was severely affected (Fig. 2). *Fgf3*$^{-/-}$/*Fgf8*$^{flox/d2,3}$; *MesP1*$^{Cre/+}$ mutants revealed only the presence of microvesicles (n=4) or complete absence of otic tissue (n=4) whereas *Fgf3*$^{-/-}$, *Fgf3*$^{-/-}$/*Fgf8*$^{flox/d2,3}$ and *Fgf8*$^{flox/d2,3}$; *MesP1*$^{Cre/+}$ mutant embryos showed formation of otic vesicles (Fig. 2A-C and data not shown). Furthermore the microvesicles failed to express the otic marker *Pax2* (Supplementary Fig. 2) and lacked *NeuroD* that labels the neurogenic region of the otic vesicle (Supplementary Fig. 3). Examination of proliferation and cell death revealed no apparent changes in the microvesicles of *Fgf3*$^{-/-}$/*Fgf8*$^{flox/d2,3}$; *MesP1*$^{Cre/+}$ embryos compared to wild-type controls at E8 and E9 (Fig. 3A,B, D,E and data not shown) .

To examine the developmental capacity of the microvesicles present in *Fgf3*$^{-/-}$/*Fgf8*$^{flox/d2,3}$; *MesP1*$^{Cre/+}$ embryos to undergo further development and differentiation, we examined these mutants at E13 (n=2). At this developmental stage microvesicles had increased in size but lacked the normal morphogenesis observed in controls (Fig. 2D,E). In 50% of cases we were unable to detect any otic tissue upon examination of serial sections at E13 through the cranial region. Therefore, the combined global loss of *Fgf3* and *Fgf8* within the mesoderm during inner ear induction results in the absence or severe reduction of otic tissue that is only able to form microvesicles that fail to undergo proper morphogenesis.

Fgf8 expression in the pharyngeal endoderm is required for the formation of a normally sized otic vesicle

The initial *Fgf8* expression in the mesoderm during otic induction is accompanied by *Fgf8* transcripts in the pharyngeal endoderm and the preplacodal surface ectoderm at E8- E9 (Fig. 1B; Ladher et al., 2005). At this stage also *Fgf3* expression is observed weakly in the pharyngeal endoderm, next to a prominent expression in the surface ectoderm and the neural tube (Fig. 1C). The *Foxa3*Cre mouse line expresses Cre recombinase from the *Foxa3* locus and has been shown to inactivate floxed alleles specifically in the pharyngeal endoderm before E8.5 (Lee et al., 2005a; Lee et al., 2005b). We confirmed Cre activity in the pharyngeal endoderm at E8.5 and in the pharyngeal pouch endoderm at E9 where *Fgf8* is expressed (Crossley et al., 1995) using ROSA26 reporter mice (Supplementary Fig. 1B,C). To obtain $Fgf3^{-/-}/Fgf8^{flox/d2,3}$; $Foxa3^{Cre/+}$ mutants we crossed $Fgf3^{+/-}/Fgf8^{d2,3/+}$;$Foxa3^{Cre/+}$ animals with $Fgf3^{-/-}/Fgf8^{flox/flox}$ mice. Upon inspection of mutant embryos at E9 we observed a reduced size of the otic vesicle compared to wild-type littermates (Fig. 4A,B). Histological sections confirmed that the size of the otic vesicle in these mutants (n=4) was also significantly reduced compared to $Fgf3^{-/-}$, $Fgf8^{flox/d2,3}$; $Foxa3^{Cre/+}$ and $Fgf3^{-/-}/Fgf8^{flox/d2,3}$ mutants (Fig. 4C-F and data not shown). Compared to wild-type embryos, the diameter and cell number of the mutant vesicles was on average reduced by 21% and 27%, respectively. Examination of proliferation (Fig. 3C) and cell death (Fig. 3F) revealed no statistically significant changes in the otic vesicles of $Fgf3^{-/-}/Fgf8^{flox/d2,3}$; $Foxa3^{Cre/+}$ mutants compared to wild-type controls (Fig. 3A,D).

To explore the developmental potential of the reduced size otic vesicles of *Fgf3*$^{-/-}$/*Fgf8*$^{flox/d2,3}$; *Foxa3*$^{Cre/+}$ embryos we examined mutant embryos at E15 (n=2). At this stage mutants had developed a normally formed inner ear as revealed by sections through the cochlea and vestibular apparatus (Fig. 4G,H and data not shown). In the cochlea at E16 we observed normal formation of supporting cells expressing Prox1 and hair cells characterized by myosin VII expression and innervation by TuJ1-positive nerve fibers (Supplementary Fig. 4). Therefore, *Fgf8* expression in the pharyngeal endoderm is required for the formation of a normally sized otic vesicle. However, the reduced size vesicle appears to maintain the capacity to undergo proper otic differentiation.

Ectopic misexpression of Fgf8 in chicken embryos affects formation of the otic vesicle

Recent studies in the chicken embryo have shown that endoderm-derived *Fgf8* initiates otic induction around HH4 (Ladher et al., 2005). *Fgf8* expression is maintained in the endoderm and is observed in the pharyngeal endoderm at HH8-10 when otic specification takes place and the placode is formed (Fig. 5A-C; Mahmood et al., 1995). Since our results in mouse embryos suggested a requirement for *Fgf8* expression in the pharyngeal endoderm we were interested if this expression domain may also be involved during otic vesicle formation in chicken embryos. We performed gain-of–function experiments by applying FGF8-soaked beads or electroporating a vector containing the *Fgf8* coding region into the surface ectoderm or neural tube of chicken embryos at HH8-HH9 (for details see Methods). Ectopic expression of *Fgf8* in the neural tube or the surface ectoderm was confirmed by RNA whole-mount *in situ* hybridization (Fig. 6A and data not shown). After incubation of embryos until the otic

vesicle stage we observed that misexpression of *Fgf8* resulted in a reduction of the size of the otic vesicle under all three experimental setups (Fig. 5D-I and 6B-E). Chicken embryos carrying beads soaked with FGF8 and implanted into the mesoderm underlying the future otic placode showed a reduced size of the otic vesicle (n=9/11) and reduced expression of *Pax2* (n=8/9) that is expressed in the medial part of the otic vesicle (Fig. 5F-I). In contrast expression of *Lmx1,* a dorsal otic marker was unaffected (Fig. 5D,E; n=2/2). Likewise, electroporation of *Fgf8* into the neural tube (n=52) or surface ectoderm (n=33) resulted in the formation of smaller sized vesicles on the electroporated side in 62,5% and 67% of the embryos, respectively, and reduced expression of otic markers (Fig. 6 and data not shown). On average the size of the otic vesicle was reduced by 28% compared to normal otic vesicles. When vectors carrying *Fgf8* were electroporated into the surface ectoderm we also often (86%) noted an increase in the size of the lens on the electroporated side (Fig. 8A and see below). Together, these data demonstrate that misexpression of *Fgf8* during otic specificiation and placode formation interferes with the development of the otic vesicle.

Misexpression of Fgf10 does not interfere with chicken otic development

During murine inner ear development *Fgf10* is expressed in the mesoderm and the developing hindbrain and has been shown to be required for otic induction (Alvarez et al., 2003; Wright and Mansour, 2003). In the chicken embryo, *Fgf10* expression has not been observed during otic induction but is present in the otic placode itself (Karabagli et al., 2002; Ohuchi et al., 1997). To examine the potential involvement of *Fgf10* during the formation of the chicken otic vesicle in we performed gain-of-function experiments identical to those described above for *Fgf8*. Beads incubated with FGF10

protein and implanted into the mesoderm underneath the future otic placode at HH8-HH9 showed no effects on formation of the otic vesicle (n=6). Likewise electroporation of vectors encoding *Fgf10* into the neural tube (n=91; Supplementary Fig. 5A) or the surface ectoderm (n=44) at this stage did not affect formation of the otic vesicle. As previously shown in murine embryos misexpression of *Fgf10* lead to the ectopic expression of *Fgf8* (Supplementary Fig. 5B, Zelarayan et al., 2007). Upon expression of *Fgf10* in the surface ectoderm we observed the formation of ectopic placodal-like structures close to the developing eye in 75% of the embryos (Fig.7). RNA in situ hybridization revealed that these structures stained for *Pax6* and *Six3*, genes characteristic for the lens and olfactory placode (Fig. 7A,B and 8B), but not for the otic marker *Pax2* (Fig. 7C). Next to these ectopic structures we also observed that the lens vesicle failed to close and expanded outside the optic cup (Fig. 8C,D), a phenotype comparable with the one observed in embryos electroporated with *Fgf8* (Fig. 8A). Therefore, ectopic *Fgf10* expression does not interfere with otic vesicle formation and although it induces placode-like structures, the ectopic tissue expresses *Pax6* and *Six3* that are not found in otic placodes.

Discussion

Unlike in chicken, *Fgf8* is not absolutely required for otic induction in mice (Ladher et al., 2005). Previous results have shown that otic induction is only affected when *Fgf8* expression is reduced on a *Fgf3* homozygous null background (Ladher et al., 2005; Zelarayan et al., 2007). Global reduction of *Fgf8* expression during otic induction was obtained by the use of a hypomorphic *Fgf8* allele ($Fgf8^{H}$) allele or mosaic inactivation of a floxed *Fgf8* allele using the *Mox2*Cre line (Ladher et al., 2005;

Zelarayan et al., 2007). However, these experiments did not provide information on the tissue-specific requirements of *Fgf8* during early inner ear development when it is expressed in several sites potentially controlling this process. By using the *MesP1*Cre line we now show that expression of *Fgf8* in the mesoderm is specifically required during otic induction. The phenotype observed in $Fgf3^{-/-}/Fgf8^{flox/d2,3}$; $MesP1^{Cre/+}$, consisting in the presence of microvesicles or absence of otic tissue, is similar to the phenotype found in $Fgf3^{-/-}/Fgf8^{flox/d2,3}$;$Mox2^{Cre/+}$ or $Fgf3^{-/-}/Fgf8^{H/-}$ mutant embryos. Therefore, reduced *Fgf8* expression in its mesodermal domain during otic induction appears to be a likely cause for the phenotype found in $Fgf3^{-/-}/Fgf8^{flox/d2,3}$;$Mox2^{Cre/+}$ or $Fgf3^{-/-}/Fgf8^{H/-}$ animals. Similar to *Fgf3*/*Fgf10* mouse mutants (Wright and Mansour, 2003) and *Fgf3/Fgf8* zebrafish mutants (Maroon et al., 2002) we found no evidence for a change in cell proliferation or cell death in $Fgf3^{-/-}/Fgf8^{flox/d2,3}$; $MesP1^{Cre/+}$ mutant embryos during otic development. However, these mutants fail to express otic markers in the otic region. Therefore, loss of FGF signalling in FGF double mutants leads to a failure to establish appropriate patterns of otic gene expression in dorsal ectoderm that consequently fails to undergo otic fate (Alvarez et al., 2003; Ladher et al., 2005; Maroon et al., 2002; Wright and Mansour, 2003; Zelarayan et al., 2007).

Next to this mesodermal domain of expression, *Fgf8* is also present during otic induction in the endoderm, where it is detected from E8 onwards. Using the *Foxa3*Cre line to specifically inactivate *Fgf8* in the endoderm on a *Fgf3* homozygous null background we observe the formation of reduced sized otic vesicles. Although Cre activity was confirmed in the endoderm it was weaker than expected based on the results obtained by Lee et al. (2005a). Nevertheless, presence of *Fgf8* is also required in the endoderm to promote the formation of a normally sized otic vesicle. A recently published *FoxA2*Cre line shows strong and specific expression in the endoderm during

early inner ear development and should help to define the role of *Fgf8* expression in the endoderm during otic induction (Frank et al., 2007).

Interestingly, we also observe *Fgf3* expression in the endoderm at E8 (6ss) prior to the so far described pattern at E.8.5 (10ss; Mahmood et al., 1996; McKay et al., 1996). Therefore next to the prominent expression in the hindbrain, *Fgf3* maybe also redundantly required together with *Fgf8* in this early endodermal domain for the formation of a normally sized otic vesicle.

At the molecular level one of the redundant functions shared between *Fgf3* and *Fgf8* is to induce or maintain normal levels of *Fgf10* in the mesoderm at E8 (Ladher et al., 2005). A similar but non-redundant requirement for endodermally expressed *Fgf8* to induce the mesodermal expression of a different *Fgf*, *Fgf19,* has been observed in the chick during the initiation of otic induction (Ladher et al., 2005). The parallel expression of *Fgf8* in the endoderm and *Fgf19* in the mesoderm is also maintained until otic specification (Kil et al., 2005; Ladher et al., 2005). To address the potential function of *Fgf8* at this stage we misexpressed it in the periotic mesoderm, neural tube and surface ectoderm. Surprisingly we observed a reduced size of the otic vesicle compared to controls under these conditions (Figs. 5 and 6). This inhibitory effect differs from the so far known functions of *Fgf8* during early chicken inner ear development when it promotes otic induction at HH6 (Ladher et al., 2005). Moreover, FGF8 beads implanted in the mesoderm next to the otic placode at later stages (HH10-11) leads to the formation of ectopic otic tissue (Adamska et al., 2001; see also Supp. Fig. 6). An explanation for these differential effects upon misexpression of Fgf8 at different timepoints may be derived from experiments in zebrafish (Hans et al., 2007). In this species *Fgf8* misexpression until midgastrula stages was shown to reduce otic tissue, probably due to a downregulation of competence factors required for otic

induction. On the other hand, misexpression during early segmentation lead to an increased size of the otic vesicle, presumably due to the induction of a larger area of competent ectoderm acquiring otic fate (Hans et al., 2007), an effect also observed upon misexpression of *Fgf3* in chick embryos (Hans et al., 2007; Vendrell et al., 2000). Interestingly, in *Xenopus* FGF8 beads have been shown to interfere with the endogenous pattern of *Fgf3* and *Fgf8* expression during midbrain development (Riou et al., 1998). Similarly in the chicken embryo, FGF8 may interfere with the function of FGFs relevant for otic development including FGF3 and FGF19 (Supplementary Fig. 6). On the other hand, sustained expression of *Fgf3* and *Fgf19* has also been shown to block otic specification in chick embryos (Freter et al., 2008). In the present context of otic development the stage-dependent differential effects of *Fgf8* thus indicate that its correct spatiotemporal expression pattern and dose is crucially required for proper otic specification and vesicle formation.

Finally, we also examined the potential function of *Fgf10* expression during early otic development by misexpressing *Fgf10* in periotic areas. *Fgf10* is the only FGF member known so far to be prominently expressed in the mouse and chicken otic placode, whereas *Fgf8* is only weakly expressed (Adamska et al., 2001; Alsina et al., 2004; Alvarez et al., 2003; Karabagli et al., 2002; Ohuchi et al., 1997; Pirvola et al., 2000). We found no effects on otic vesicle development upon misexpression of *Fgf10* from different tissue sources in chicken embryos. In contrast, misexpression of *Fgf10* in the neural tube of mouse embryos during otic induction leads to the formation of ectopic vesicles (Alvarez et al., 2003). This result demonstrated that *Fgf10* acting form the neural tube may induce otic fate, possibly reflecting a endogenous function of *Fgf10* during its expression in the neural tube throughout otic induction (Alvarez et al., 2003).

Upon electroporation of *Fgf8* and *Fgf10* into the surface ectoderm we also observed defects during lens development. The size of the lens tissue was increased and the forming lens vesicle frequently failed to close. A similar phenotype has been reported upon the implantation of FGF8 beads next to the optic vesicle in chicken embryos (Kurose et al., 2005; Vogel-Hopker et al., 2000). Additionally, upon misexpression of *Fgf10* we observed the formation of ectopic placodal-like tissue characterized by the expression of markers present in the lens placode, whereas the otic marker *Pax2* failed to stain the ectopic structures. The ectopic tissue formed may thus correspond to ectopic lens tissue. Alternatively, the structures may possibly be also related to the initiation of ectopic lacrimal buds that are also characterized by *Pax6* expression and have been shown to be induced upon implantation of FGF10-soaked beads into the periocular mesenchyme in mice and are absent in *Fgf10* mutants (Entesarian et al., 2005; Makarenkova et al., 2000).

Experimental Procedures

Transgenic mice

The following mouse lines used in this study have been described previously: *Fgf3*$^{-/-}$ knockout mutants and mutants carrying a conditional (*Fgf8*^{flox}) or a null allele (*Fgf8*^{d2,3}) for *Fgf8* (Meyers et al., 1998), the ROSA26 Cre reporter strain (Soriano, 1999) and mouse lines in which *cre* has either been targeted to the *Foxa3* (Lee et al., 2005b) or *MesP1* (Saga et al., 1999) locus.

Histology and RNA in situ hybridization

Preparation of histological sections stained with hematoxylin and eosin, RNA whole-mount in situ hybridisation, β-galactosidase staining and the sectioning of stained embryos has been described previously (Alvarez et al., 2003). The riboprobe corresponding to chicken *Fgf8* and mouse *NeuroD* have been described (Crossley and Martin, 1995; Vazquez-Echeverria et al., 2008). All other riboprobes used in this study have been referred to previously (Alvarez et al., 2003; Vendrell et al., 2000; Zelarayan et al., 2007). Measurements of otic vesicle diameters and cell counts were performed on serial sections. For immunohistochemistry cryostat sections were prepared and processed as outlined earlier (Carnicero et al., 2004). Prox1 (Covance, diluted 1:100), myosin VIIA (Proteus, diluted 1:100) and TuJ1 (Covance, diluted 1:1000) antibodies were used.

Detection of proliferating cells and cell death

Detection of cell proliferation in sections was performed by immunohistochemistry using the anti-phosphorylated histone H3 antibody (rabbit polyclonal Phospho H3 from Upstate Biotechnology, USA) diluted at 1/100. TUNEL analysis was performed using an in situ cell death detection kit following the manufacturer´s recommendations (Roche).

Manipulation of chick embryos

Heparin acrylic beads (Sigma, H5263) were soaked for at least 1 hr at room temperature in recombinant mouse FGF8 or FGF10 (0.5 mg/ml from R&D Systems) and implanted at stage HH8-9 (Hamburger and Hamilton, 1992) into the mesoderm underlying the area where the otic placode is specified in the surface ectoderm. For in ovo electroporation, embryos were incubated until stage HH8-9. The solution containing the different plasmids encoding either murine *Fgf8* or *Fgf10* cDNA (cloned into pCS2) plus a GFP reporter plasmid pLP-EGFP-C1 (Clontech) at 0.8 μg/μl in PBS, was injected into the lumen of the neural tube or placed as an overlay on top of the embryo with a glass microcapillary. Two parallel platinum electrodes (0.5 mm width and 4 mm length) with a distance of 5 mm between them were positioned on both sides of the embryo. Subsequently 4 pulses of 30 V of 50 msec duration each and an interval of 1 msec were applied using a BTX electroporator. Embryos were incubated until the otic vesicle stage and then processed for histology or stained with riboprobes. Control experiments included electroporation of the GFP or *lacZ* reporter plasmid (Supplementary Fig. 7).

Acknowledgments

We thank Gail Martin for *Fgf8* mutant mouse lines, Maria Teresa Alonso for helpful discussions and Yesica Gaciño and Diana Zatua for technical support. Mouse lines in which *cre* has either been targeted to the *Foxa3* or *MesP1* locus were obtained from the MMRRC and the RIKEN BRC, respectively. Supported by the Spanish MiCINN (BFU2007-61030), TerCel, Ciberned, Junta de Castilla y León and the DFG (SFB 444).

Figure Legends

Figure 1

Expression of *Fgf8* and *Fgf3* in tissues relevant for otic induction. (A-C) Embryos have been hybridized with a *Fgf8* or *Fgf3* riboprobe and sectioned transversally at the level where inner ear induction takes place. (A) At E7.5 *Fgf8* is strongly expressed in the mesoderm (m). (B) At E8 *Fgf8* is expressed in the pharyngeal endoderm (e), mesoderm and surface ectoderm (se), whereas *Fgf3* (C) is found in the neural tube (nt), surface ectoderm and weakly in the endoderm. The orientation of the sections along the dorsal (D)-ventral (V) axis are indicated in (A). Scale bars, in A, 50 μm for A, 100 μm for B,C.

Figure 2

Inner ear phenotype of $Fgf3^{-/-}/Fgf8^{flox/d2,3};MesP1^{Cre/+}$ mutants. (A-C) Histological sections through the otic vesicle of $Fgf3^{-/-}$ (A), $Fgf8^{flox/d2,3};MesP1^{Cre/+}$ (B) and $Fgf3^{-/-}/Fgf8^{flox/d2,3};MesP1^{Cre/+}$ (C) embryos at E9. Note the microvesicle distant from the neural tube present in $Fgf3^{-/-}/Fgf8^{flox/d2,3};MesP1^{Cre/+}$ mutant embryos. (D, E) Histological sections through the inner ear of wild-type (wt) and $Fgf3^{-/-}/Fgf8^{flox/d2,3};MesP1^{Cre/+}$ mutant embryos at E13. (D) In the wild-type embryo the developing cochlea (co), saccule (s), endolymphatic duct (ed) and the posterior (pc) and lateral semicircular canal (lc) are indicated. (E) Sections of the mutant embryo reveal only the presence of a small undifferentiated otic vesicle with a lateral protuberance. The orientation of the sections

along the dorsal (D)-lateral (L) axis are indicated in (A). Scale bars: in A, 60 μm for A-C and in D, 225 μm for D and E.

Figure 3

Cell proliferation and cell death in otic vesicles of *Fgf3*$^{-/-}$/*Fgf8*$^{flox/d2,3}$;*MesP1*$^{Cre/+}$ and *Fgf3*$^{-/-}$/*Fgf8*$^{flox/d2,3}$;*Foxa3*$^{Cre/+}$ mutant embryos at E9. (A-C) Cell proliferation was examined by staining sections at the level of the otic vesicle with antibodies raised against phospho-Histone 3. Note the presence of proliferating cells in wild-type (A) and *Fgf3/Fgf8* double mutant embryos with the indicated genotypes (B,C). (D-F) Cell death was analysed by TUNEL staining of the otic area. Note the presence of apoptotic cells in wild-type (D), *Fgf3*$^{-/-}$/*Fgf8*$^{flox/d2,3}$;*MesP1*$^{Cre/+}$ (E) and *Fgf3*$^{-/-}$/*Fgf8*$^{flox/d2,3}$;*Foxa3*$^{Cre/+}$ (F) mutant embryos. The circumference of the microvesicle in *Fgf3*$^{-/-}$/*Fgf8*$^{flox/d2,3}$;*MesP1*$^{Cre/+}$ mutants is indicated by a stippled line. The orientation of the sections along the dorsal (D)-lateral (L) axis are indicated in (A). Scale bars: in A, 100 μm for A-F.

Figure 4

Inner ear phenotype of *Fgf3*$^{-/-}$/*Fgf8*$^{flox/d2,3}$;*Foxa3*$^{Cre/+}$ mutants. (A,B) External appearance of wild-type (wt) and *Fgf3*$^{-/-}$/*Fgf8*$^{flox/d2,3}$;*Foxa3*$^{Cre/+}$ mutant embryos at E9. The otic vesicle is indicated by an arrow. (C-F) Histological sections through the otic vesicle of wild-type (C), *Fgf3*$^{-/-}$ (D), *Fgf8*$^{flox/d2,3}$;*Foxa3*$^{Cre/+}$ (E) and *Fgf3*$^{-/-}$/*Fgf8*$^{flox/d2,3}$;*Foxa3*$^{Cre/+}$ (F) embryos at E9. Note the reduced size of the otic vesicle in *Fgf3*$^{-/-}$/*Fgf8*$^{flox/d2,3}$;*Foxa3*$^{Cre/+}$ mutant embryos. Histological sections at E15 reveal the presence of a normal cochlea in *Fgf3*$^{-/-}$/*Fgf8*$^{flox/d2,3}$;*Foxa3*$^{Cre/+}$ mutants compared to wild-type

animals. Abbreviations: cg, cochlear ganglion; se, sensory epithelium. The orientation of the sections along the dorsal (D)-lateral (L) axis are indicated in (C). Scale bars: in C, 100 μm for C-F, 400 μm for G,H.

Figure 5

Phenotype of chicken embryos upon implantation of FGF8 beads. (A,B) Chicken embryos hybridised with a riboprobe for *Fgf8* at the 7ss (A) and 10ss (B). The pharyngeal endoderm is indicated with an arrow. (C) Transversal section of the embryo shown in (B) at the level of the otic placode (op). Note expression of *Fgf8* in the pharyngeal endoderm (e). (D-G) Chicken embryos with beads, previously soaked in PBS (D,F) or FGF8 protein (E,G) and then implanted in the prospective otic region at HH8, were incubated for 40 hours and stained with a riboprobe for *Lmx1* (D,E) or *Pax2* (F,G), respectively. Note the reduced size of the otic vesicles in the embryos carrying the FGF8 bead and loss of staining for *Pax2* (G) whereas *Lmx1* expression is maintained (E). Orientation of the embryos along the anterior (A)- dorsal (D) axis is indicated in (D). (H, I) Sections through the otic vesicle of embryos shown in (F) and (G). The circumference of the otic vesicles are indicated by stippled lines. Orientation of the sections along the dorsal (D)- lateral (L) axis are indicated. Scale bars: in C, 200 μm and in I, 100 μm for H,I.

Figure 6

Phenotype of chicken embryos upon electroporation of *Fgf8* into the neural tube. (A) Chicken embryo electroporated with a vector encoding murine *Fgf8* at HH8 and stained with a murine *Fgf8* riboprobe at HH15. (B,C) Aspect of the electroporated (B) and unelectroporated side (C) of a chicken embryo 36 hours after electroporation of a vector encoding *Fgf8* into the neural tube at HH8. Orientation of the embryo along the dorsal (d)- anterior (a) axis is indicated. (D) Transversal section through a *Fgf8*-electroporated embryo. Note that on the electroporated right side the size of the otic vesicle is reduced. (E) Transversal section of a *Fgf8*-electroporated embryo stained with a *Pax2* riboprobe. Note the reduced size and *Pax2* staining of the otic vesicle on the electroporated right side of the embryo. Orientation of the embryos in (D) and (E) along the dorsal (d)-lateral (l) axis is indicated in (D). Scale bars: in D, 40 μm and in E, 100 μm.

Figure 7

Phenotype of chicken embryos upon misexpression of *Fgf10*. (A-C) Chicken embryos were electroporated at HH8 into the surface ectoderm with a vector encoding *Fgf10*, incubated for 40 hours and stained with the indicated riboprobes. Note the presence of vesicular structures that are stained with a *Pax6* (A) and *Six3* (B) riboprobe but lack *Pax2* staining (C, arrow). (D-F) Expression of the indicated genes in control embryos.

Figure 8

Lens phenotypes of embryos electroporated with *Fgf8* or *Fgf10*. Embryos were electroporated at HH8 in the surface ectoderm and incubated for 40 hours. (A) External appearance of a control embryo (left) and an embryo electroporated with a vector encoding *Fgf8* (right). Note the increased size of the lens vesicle of the electroporated embryo indicated by an arrow. (B) Section of an embryo electroporated with *Fgf10.* An ectopic placodal-like structure (arrow) stained with a riboprobe for *Six3* and the expanded lens vesicle (lv) are indicated. (C,D) Section through the unelectroporated (C) and *Fgf10*-electroporated side (D) side of an embryo stained with *Six3*. Note that on the electroporated side the lens vesicle has failed to close and expands outside of the optic cup (oc). Scale bar: in B corresponds to 25 μm, and to 50 μm for C,D.

Supplementary Figure 1

Expression of Cre controlled by the *MesP1* and *Foxa3* locus in tissues relevant for inner ear formation. Embryos have been stained for *lacZ* and sectioned transversally at the level where inner formation takes place. (A) As revealed by *lacZ* staining of a $R26R^{lacZ/+}$; $Mesp1^{Cre/+}$ embryo at E7.75 Cre controlled by the *Mesp1* locus is expressed in the mesoderm (m) but not in the pharyngeal endoderm (e). As revealed by *lacZ* staining of a $R26R^{lacZ/+}$; $Foxa3^{Cre/+}$ embryo Cre controlled by the *Foxa3* locus is expressed in the pharyngeal endoderm (e) at E8.5 (B) and pharyngeal pouch endoderm (pe) at E9 (C) but not in the mesoderm (m). Abbreviations: op, otic placode; ov, otic vesicle. Scale bar in A, 100 μm for A-C.

Supplementary Figure 2

Expression of *Pax2* in wild-type and *Fgf3*$^{-/-}$/*Fgf8*$^{flox/d2,3}$;*MesP1*$^{Cre/+}$ mutants. Sections through the otic region of a wild-type (A) and a *Fgf3*$^{-/-}$/*Fgf8*$^{flox/d2,3}$;*MesP1*$^{Cre/+}$ mutant (B) embryo at E9 hybridised with the otic marker *Pax2*. Whereas normal expression of *Pax2* localized to the medial part of the otic vesicle (ov) is observed in the wild-type embryo, the microvesicle formed in the mutant embryo (indicated by a stippled line) lacks *Pax2* expression. The orientation of the sections along the medial (M)-lateral (L) axis are indicated in (A). Abbreviation: nt, neural tube. Scale bars: in A, 100 μm for A, B.

Supplementary Figure 3

Expression of *NeuroD* in wild-type (A) and *Fgf3*$^{-/-}$/*Fgf8*$^{flox/d2,3}$;*MesP1*$^{Cre/+}$ mutants (B) at E10. Neuronal precursors corresponding to the trigeminal (V), facial (VII), otic (VII), glossopharyngeal (IX) and vagal (X) ganglia are indicated. Note the absence of *NeuroD* expression in the neurogenic region of the otic vesicle (indicated by stippled lines) and reduced labelling of the facial ganglion in the *Fgf3*$^{-/-}$/*Fgf8*$^{flox/d2,3}$;*MesP1*$^{Cre/+}$ mutant.

Supplementary Figure 4

Formation of the cochlear sensory epithelium in *Fgf3*$^{-/-}$/*Fgf8*$^{flox/d2,3}$;*Foxa3*$^{Cre/+}$ mutant embryos. Sections through the cochlear sensory epithelium reveal the presence of myosin VIIA-positive hair cells (red) innervated by nerve fibers labelled with TuJ1

(green) and Prox1-positive supporting cells (red) in wild-type (A,C) and mutant (B,D) embryos at E16. Scale bars: in A, 10 μm for A-D.

Supplementary Figure 5

Misexpression of *Fgf10* in the neural tube of chicken embryos. (A) Embryo electroporated with a vector expressing murine *Fgf10* into the left part of the neural tube at HH8 and stained with a riboprobe for mouse *Fgf10* at HH14. (B) Embryo electroporated into the left part of the neural tube with a vector expressing murine *Fgf10* in rhombomeres 3 (r3) and r5 (Zelarayan et al., 2007) at HH8 and stained with a riboprobe for chicken *Fgf8* at HH10.

Supplementary Figure 6

Model for explaining the differential effects upon ectopic FGF8 expression during early inner ear development. Schematic sections of chicken embryos taken at the level where inner ear induction and otic placode formation takes place. Ectopic expression of FGF8 at HH8, in this case indicated by beads placed in the mesoderm (m), interferes (red flashes) with the action of other FGFs, like *Fgf3* or *Fgf19* that are present in the neural tube (n) and/or mesoderm (m) and are known to stimulate otic placode formation (blue arrows) in the preplacodal ectoderm (pp). The interference of FGF8 with other FGFs may also take place indirectly caused by the downregulation of competence factors (see main text). At HH10 when the otic placode (op) has formed, ectopic FGF8 expression leads to an increased size of the otic vesicle, presumably due to a larger area of competent ectoderm acquiring otic fate.

Supplementary Figure 7

Normal development of chicken embryos electroporated with control vectors. (A) Chicken embryo electroporated with a vector expressing *gfp* at HH8 in the neural tube (nt) and left to develop for 36 hours. Formation of the otic vesicle (ov) whose circumference is indicated by a stippled line is unaffected. (B) Embryo electroporated at HH8 in the surface ectoderm with a vector encoding *β*-galactosidase and incubated for 40 hours. Formation of the lens vesicle (lv) expressing *lacZ* is unaffected.

References

Adamska, M., Herbrand, H., Adamski, M., Kruger, M., Braun, T. and Bober, E. (2001) FGFs control the patterning of the inner ear but are not able to induce the full ear program. Mech Dev 109, 303-13.

Alsina, B., Abello, G., Ulloa, E., Henrique, D., Pujades, C. and Giraldez, F. (2004) FGF signaling is required for determination of otic neuroblasts in the chick embryo. Dev Biol 267, 119-34.

Alvarez, Y., Alonso, M.T., Vendrell, V., Zelarayan, L.C., Chamero, P., Theil, T., Bosl, M.R., Kato, S., Maconochie, M., Riethmacher, D. and Schimmang, T. (2003) Requirements for FGF3 and FGF10 during inner ear formation. Development 130, 6329-38.

Bailey, A.P. and Streit, A. (2006) Sensory organs: making and breaking the pre-placodal region. Curr Top Dev Biol 72, 167-204.

Carnicero, E., Zelarayan, L.C., Ruttiger, L., Knipper, M., Alvarez, Y., Alonso, M.T. and Schimmang, T. (2004) Differential roles of fibroblast growth factor-2 during development and maintenance of auditory sensory epithelia. J Neurosci Res 77, 787-97.

Crossley, P.H. and Martin, G.R. (1995) The mouse Fgf8 gene encodes a family of polypeptides and is expressed in regions that direct outgrowth and patterning in the developing embryo. Development 121, 439-51.

Entesarian, M., Matsson, H., Klar, J., Bergendal, B., Olson, L., Arakaki, R., Hayashi, Y., Ohuchi, H., Falahat, B., Bolstad, A.I., Jonsson, R., Wahren-Herlenius, M. and Dahl, N. (2005) Mutations in the gene encoding fibroblast growth factor 10 are associated with aplasia of lacrimal and salivary glands. Nat Genet 37, 125-7.

Frank, D.U., Elliott, S.A., Park, E.J., Hammond, J., Saijoh, Y. and Moon, A.M. (2007) System for inducible expression of cre-recombinase from the Foxa2 locus in endoderm, notochord, and floor plate. Dev Dyn 236, 1085-92.

Freter, S., Muta, Y., Mak, S.S., Rinkwitz, S. and Ladher, R.K. (2008) Progressive restriction of otic fate: the role of FGF and Wnt in resolving inner ear potential. Development 135, 3415-24.

Groves, A.K. (2005) The induction of the otic placode. In Kelley, M.W., Wu, D.K., Popper, and A.N., F., R.R. (eds.), Development of the Inner Ear, Springer, New York, pp. pp. 10-42.

Groves, A.K. and Bronner-Fraser, M. (2000) Competence, specification and commitment in otic placode induction. Development 127, 3489-99.

Hamburger, V. and Hamilton, H.L. (1992) A series of normal stages in the development of the chick embryo. 1951. Dev Dyn 195, 231-72.

Hans, S., Christison, J., Liu, D. and Westerfield, M. (2007) Fgf-dependent otic induction requires competence provided by Foxi1 and Dlx3b. BMC Dev Biol 7, 5.

Hidalgo-Sanchez, M., Alvarado-Mallart, R. and Alvarez, I.S. (2000) Pax2, Otx2, Gbx2 and Fgf8 expression in early otic vesicle development. Mech Dev 95, 225-9.

Karabagli, H., Karabagli, P., Ladher, R.K. and Schoenwolf, G.C. (2002) Comparison of the expression patterns of several fibroblast growth factors during chick gastrulation and neurulation. Anat Embryol (Berl) 205, 365-70.

Kil, S.H., Streit, A., Brown, S.T., Agrawal, N., Collazo, A., Zile, M.H. and Groves, A.K. (2005) Distinct roles for hindbrain and paraxial mesoderm in the induction

and patterning of the inner ear revealed by a study of vitamin-A-deficient quail. Dev Biol 285, 252-71.
Kurose, H., Okamoto, M., Shimizu, M., Bito, T., Marcelle, C., Noji, S. and Ohuchi, H. (2005) FGF19-FGFR4 signaling elaborates lens induction with the FGF8-L-Maf cascade in the chick embryo. Dev Growth Differ 47, 213-23.
Ladher, R.K., Wright, T.J., Moon, A.M., Mansour, S.L. and Schoenwolf, G.C. (2005) FGF8 initiates inner ear induction in chick and mouse. Genes Dev 19, 603-13.
Lee, C.S., Friedman, J.R., Fulmer, J.T. and Kaestner, K.H. (2005a) The initiation of liver development is dependent on Foxa transcription factors. Nature 435, 944-7.
Lee, C.S., Sund, N.J., Behr, R., Herrera, P.L. and Kaestner, K.H. (2005b) Foxa2 is required for the differentiation of pancreatic alpha-cells. Dev Biol 278, 484-95.
Mahmood, R., Kiefer, P., Guthrie, S., Dickson, C. and Mason, I. (1995) Multiple roles for FGF-3 during cranial neural development in the chicken. Development 121, 1399-410.
Mahmood, R., Mason, I.J. and Morriss-Kay, G.M. (1996) Expression of Fgf-3 in relation to hindbrain segmentation, otic pit position and pharyngeal arch morphology in normal and retinoic acid-exposed mouse embryos. Anat Embryol (Berl) 194, 13-22.
Makarenkova, H.P., Ito, M., Govindarajan, V., Faber, S.C., Sun, L., McMahon, G., Overbeek, P.A. and Lang, R.A. (2000) FGF10 is an inducer and Pax6 a competence factor for lacrimal gland development. Development 127, 2563-72.
Maroon, H., Walshe, J., Mahmood, R., Kiefer, P., Dickson, C. and Mason, I. (2002) Fgf3 and Fgf8 are required together for formation of the otic placode and vesicle. Development 129, 2099-108.
McKay, I.J., Lewis, J. and Lumsden, A. (1996) The role of FGF-3 in early inner ear development: an analysis in normal and kreisler mutant mice. Dev Biol 174, 370-8.
Meyers, E.N., Lewandoski, M. and Martin, G.R. (1998) An Fgf8 mutant allelic series generated by Cre- and Flp-mediated recombination. Nat Genet 18, 136-41.
Ohuchi, H., Nakagawa, T., Yamamoto, A., Araga, A., Ohata, T., Ishimaru, Y., Yoshioka, H., Kuwana, T., Nohno, T., Yamasaki, M., Itoh, N. and Noji, S. (1997) The mesenchymal factor, FGF10, initiates and maintains the outgrowth of the chick limb bud through interaction with FGF8, an apical ectodermal factor. Development 124, 2235-44.
Park, E.J., Ogden, L.A., Talbot, A., Evans, S., Cai, C.L., Black, B.L., Frank, D.U. and Moon, A.M. (2006) Required, tissue-specific roles for Fgf8 in outflow tract formation and remodeling. Development 133, 2419-33.
Pirvola, U., Spencer-Dene, B., Xing-Qun, L., Kettunen, P., Thesleff, I., Fritzsch, B., Dickson, C. and Ylikoski, J. (2000) FGF/FGFR-2(IIIb) signaling is essential for inner ear morphogenesis. J Neurosci 20, 6125-34.
Riou, J.F., Delarue, M., Mendez, A.P. and Boucaut, J.C. (1998) Role of fibroblast growth factor during early midbrain development in Xenopus. Mech Dev 78, 3-15.
Saga, Y., Miyagawa-Tomita, S., Takagi, A., Kitajima, S., Miyazaki, J. and Inoue, T. (1999) MesP1 is expressed in the heart precursor cells and required for the formation of a single heart tube. Development 126, 3437-47.
Schimmang, T. (2007) Expression and functions of FGF ligands during early otic development. Int J Dev Biol 51, 473-81.
Soriano, P. (1999) Generalized lacZ expression with the ROSA26 Cre reporter strain. Nat Genet 21, 70-1.

Stolte, D., Huang, R. and Christ, B. (2002) Spatial and temporal pattern of Fgf-8 expression during chicken development. Anat Embryol (Berl) 205, 1-6.

Vazquez-Echeverria, C., Dominguez-Frutos, E., Charnay, P., Schimmang, T. and Pujades, C. (2008) Analysis of mouse kreisler mutants reveals new roles of hindbrain-derived signals in the establishment of the otic neurogenic domain. Dev Biol 322, 167-78.

Vendrell, V., Carnicero, E., Giraldez, F., Alonso, M.T. and Schimmang, T. (2000) Induction of inner ear fate by FGF3. Development 127, 2011-9.

Vogel-Hopker, A., Momose, T., Rohrer, H., Yasuda, K., Ishihara, L. and Rapaport, D.H. (2000) Multiple functions of fibroblast growth factor-8 (FGF-8) in chick eye development. Mech Dev 94, 25-36.

Wright, T.J. and Mansour, S.L. (2003) Fgf3 and Fgf10 are required for mouse otic placode induction. Development 130, 3379-90.

Zelarayan, L.C., Vendrell, V., Alvarez, Y., Dominguez-Frutos, E., Theil, T., Alonso, M.T., Maconochie, M. and Schimmang, T. (2007) Differential requirements for FGF3, FGF8 and FGF10 during inner ear development. Dev Biol 308, 379-91.

Figure 1

Click here to download high resolution image

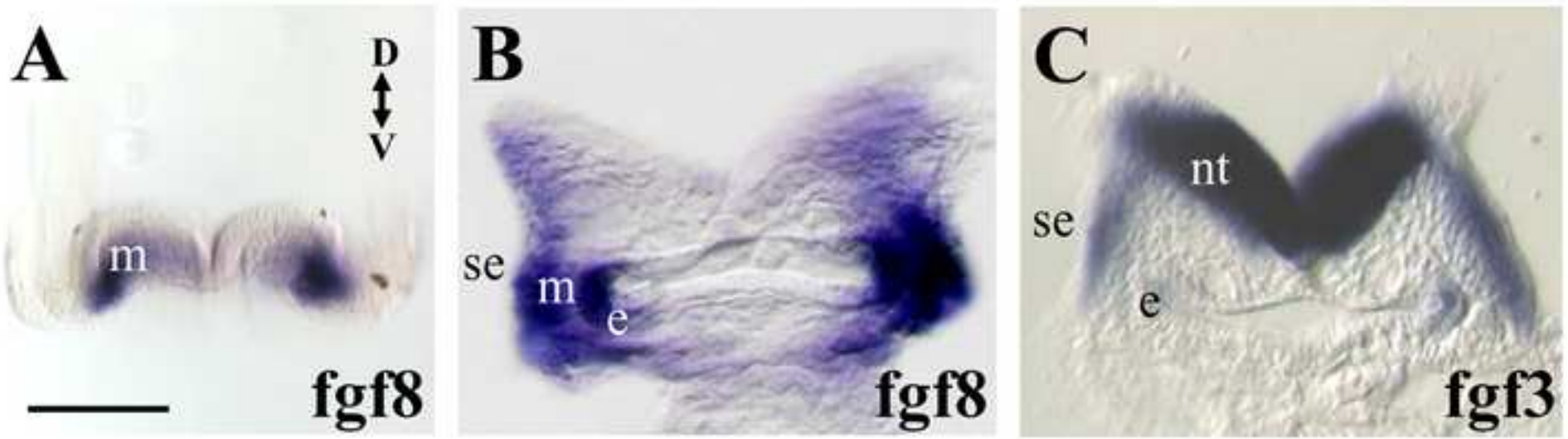

Figure 2

Click here to download high resolution image

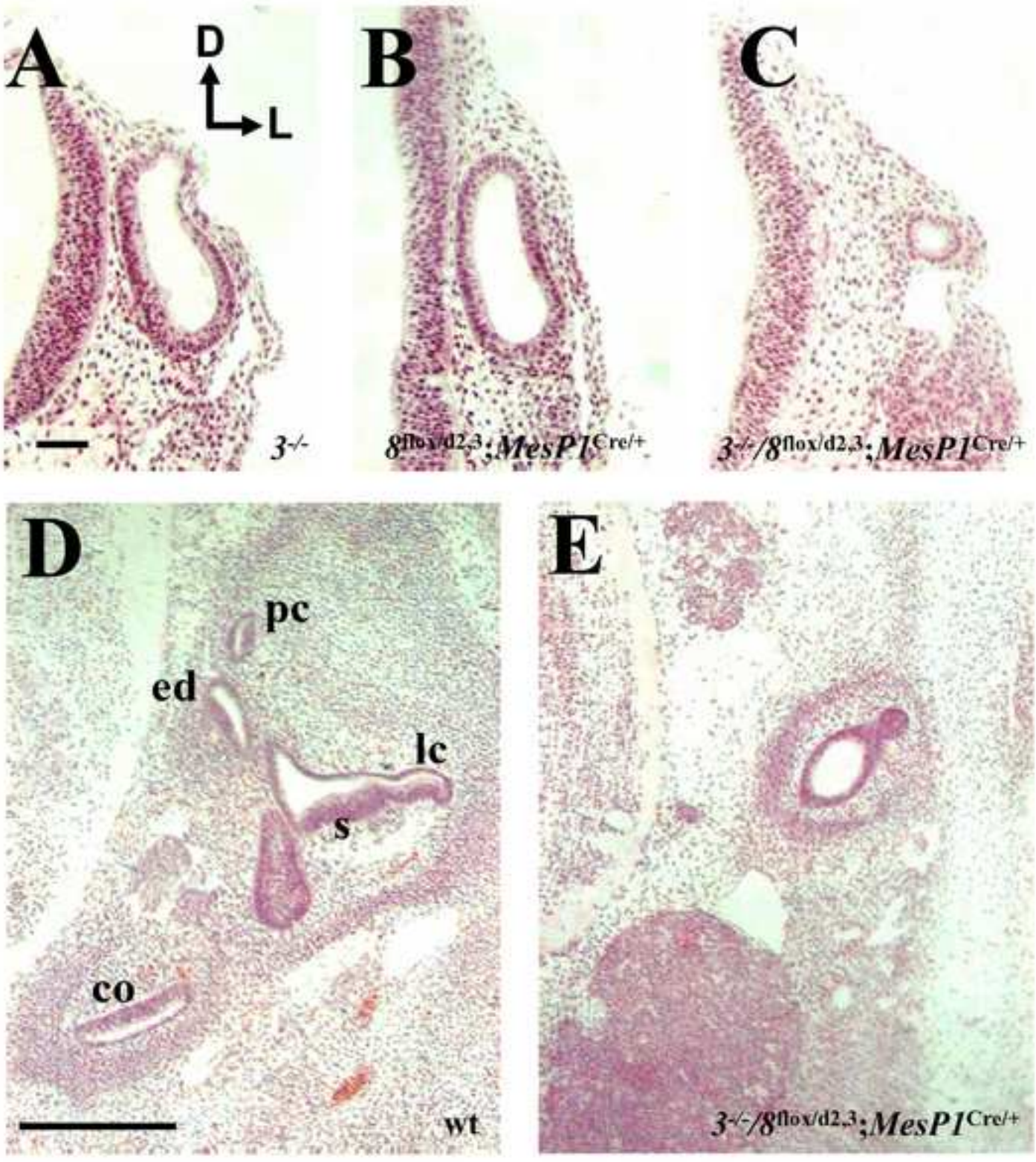

Figure 3

Click here to download high resolution image

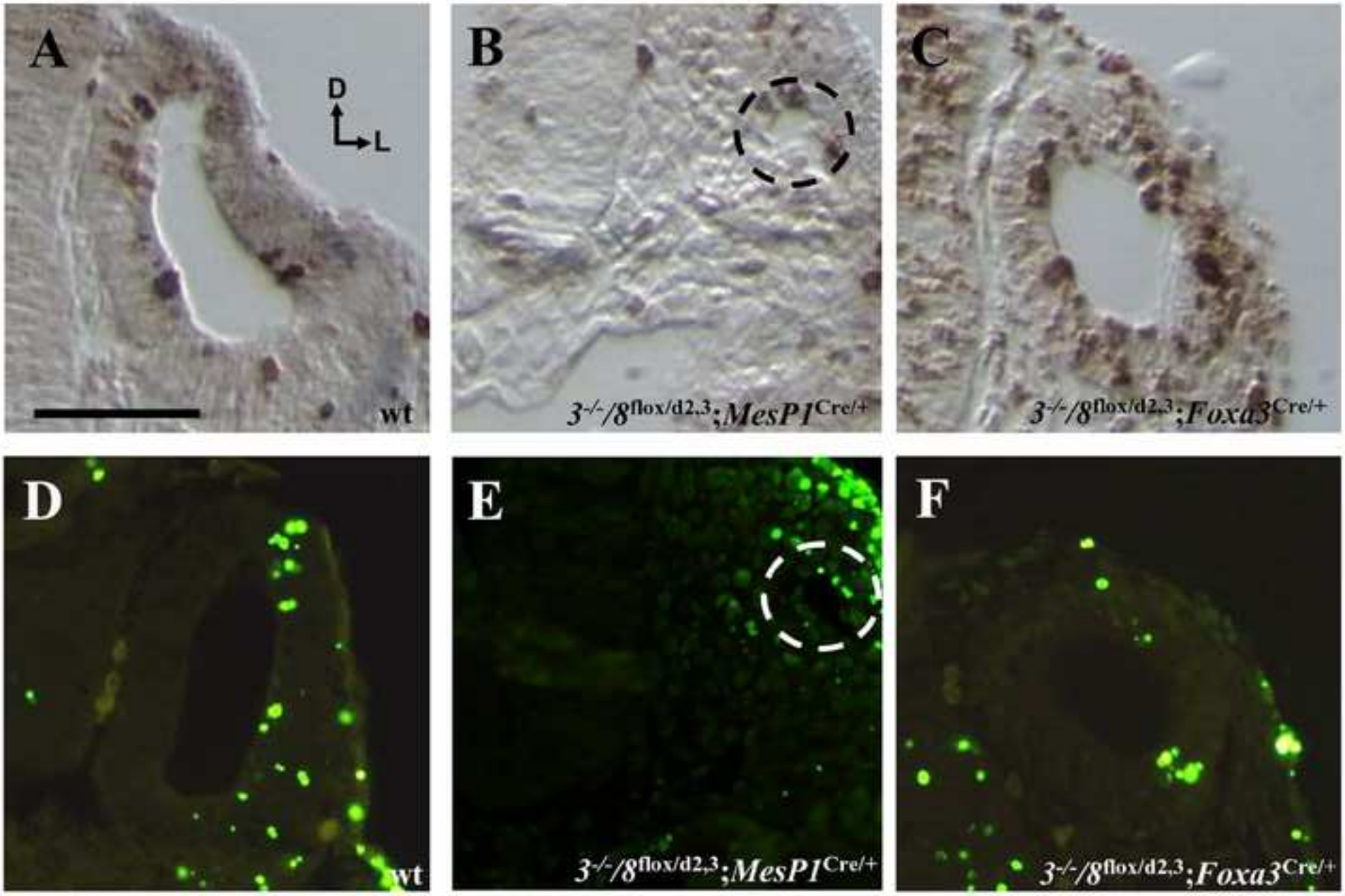

Figure 4

Click here to download high resolution image

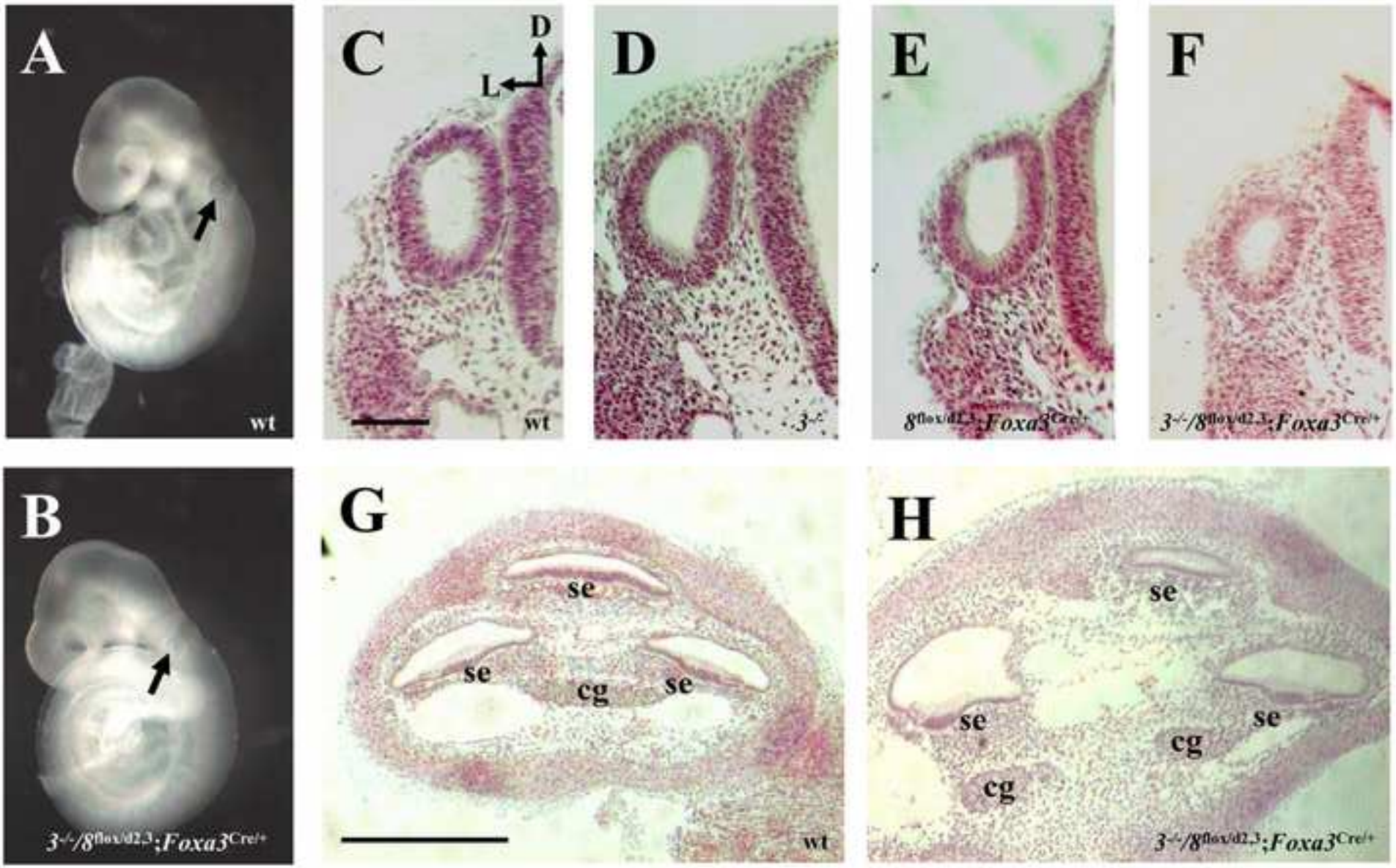

Figure 5

Click here to download high resolution image

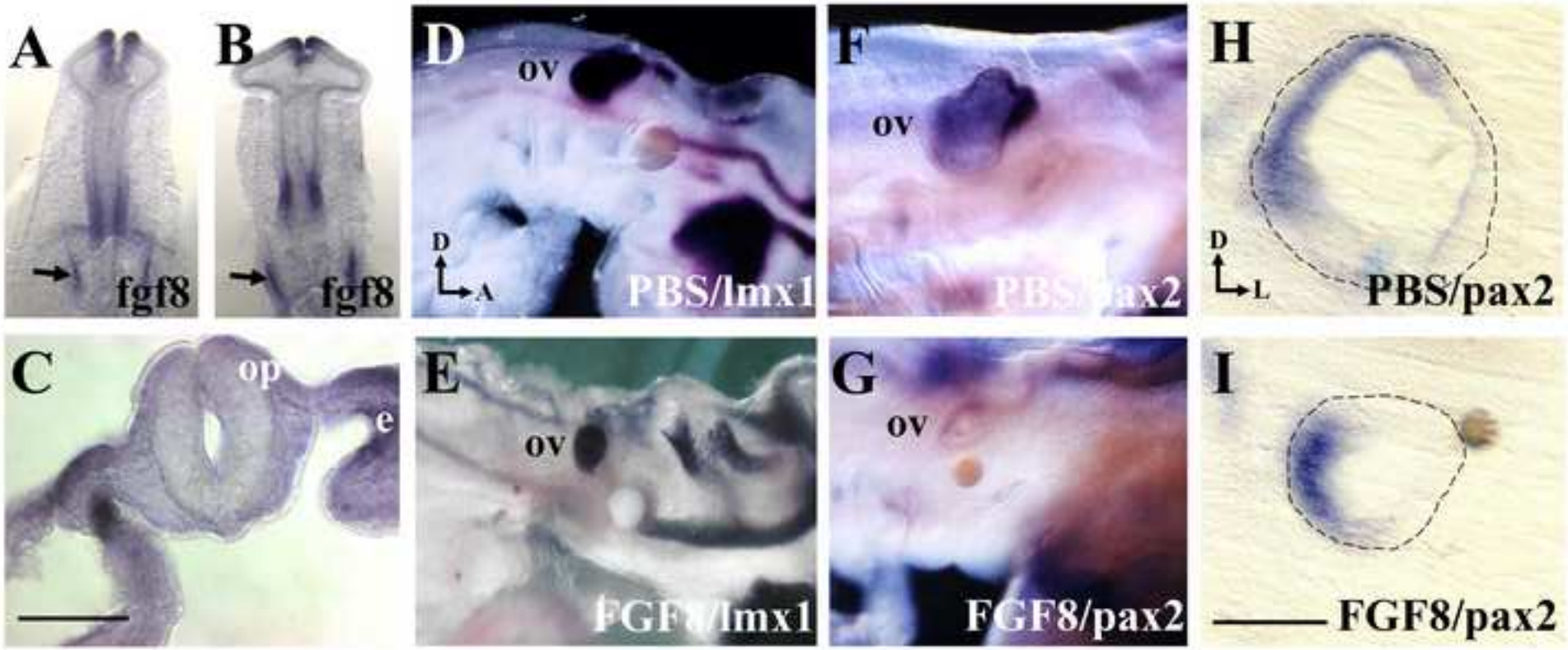

Figure 6

Click here to download high resolution image

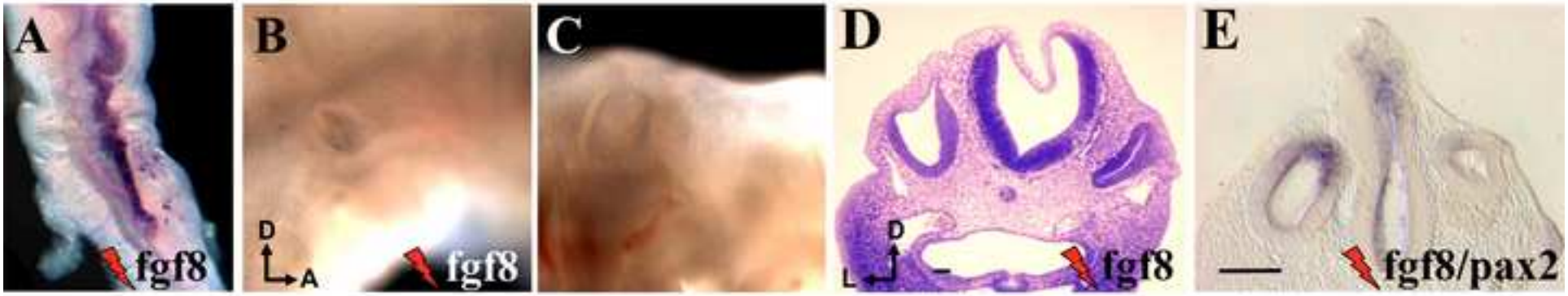

Figure 7

Click here to download high resolution image

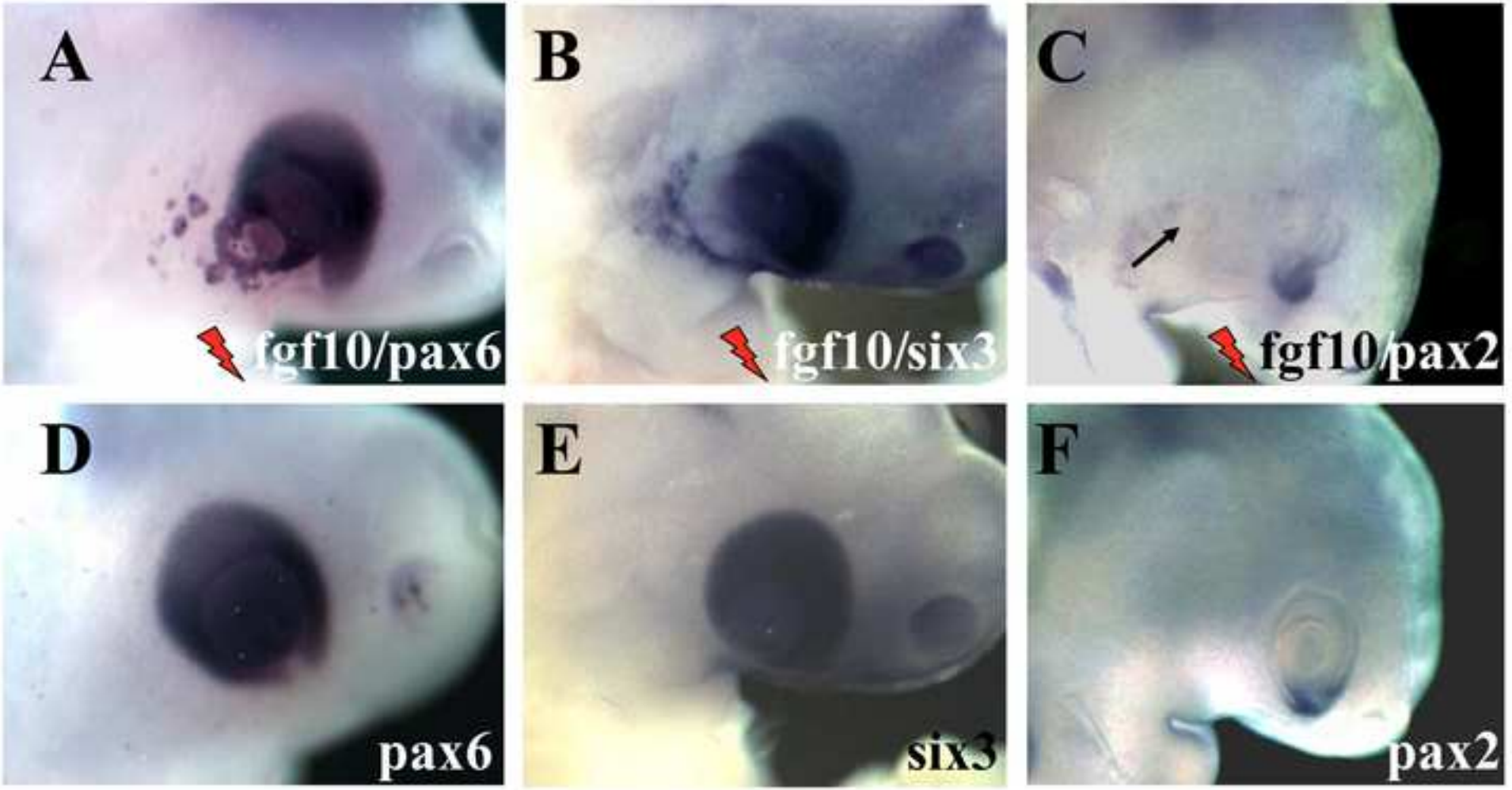

Figure 8

Click here to download high resolution image

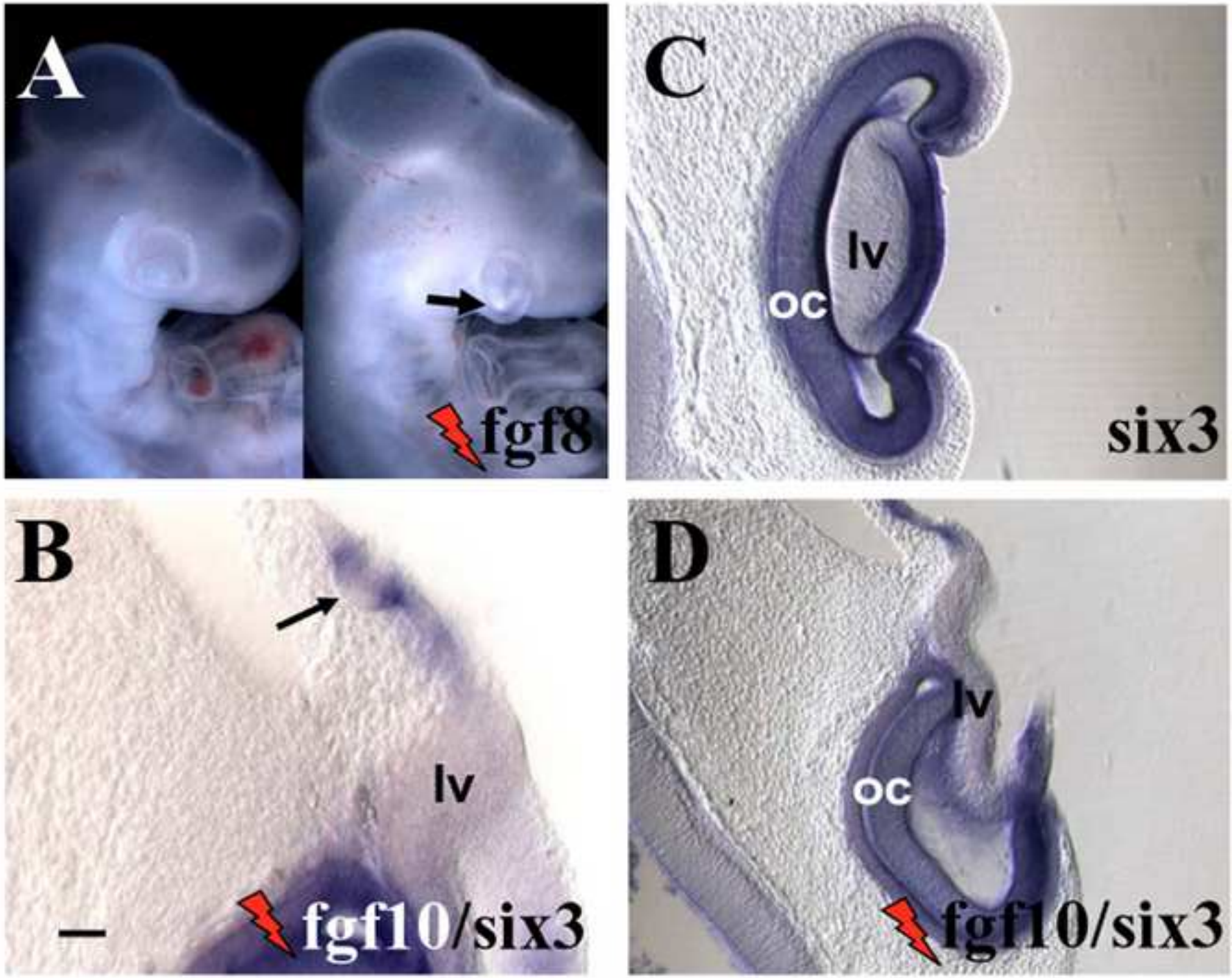

Supplementary Figure 1

Click here to download high resolution image

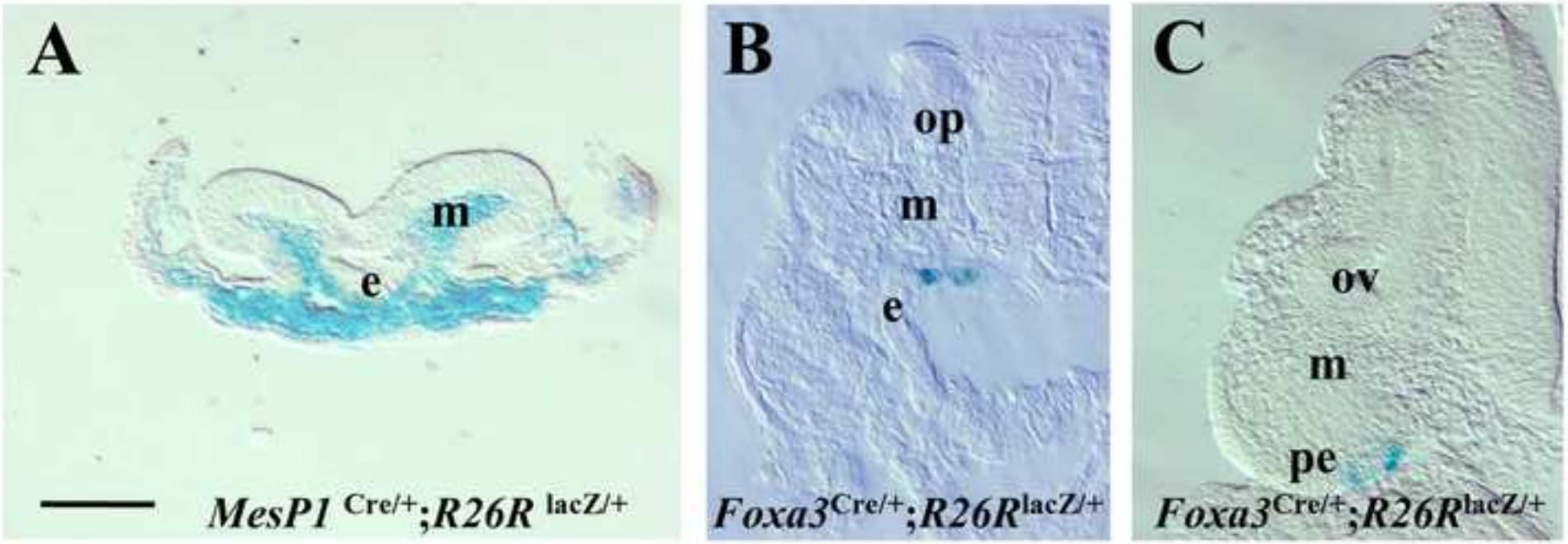

Supplementary Figure 2

Click here to download high resolution image

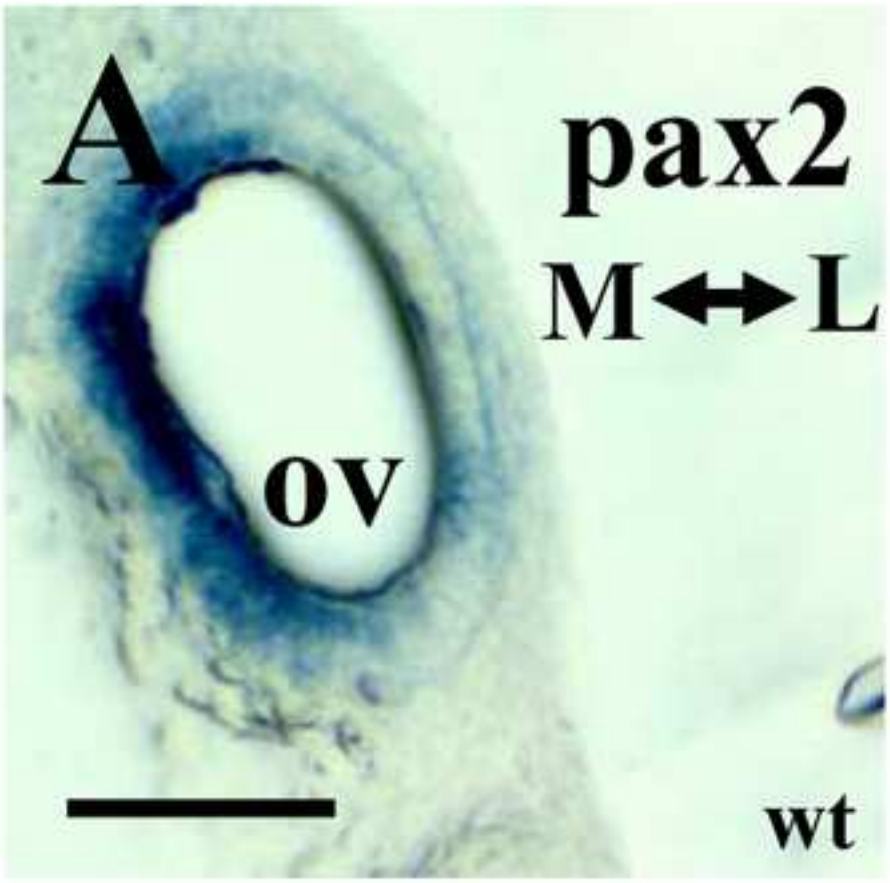

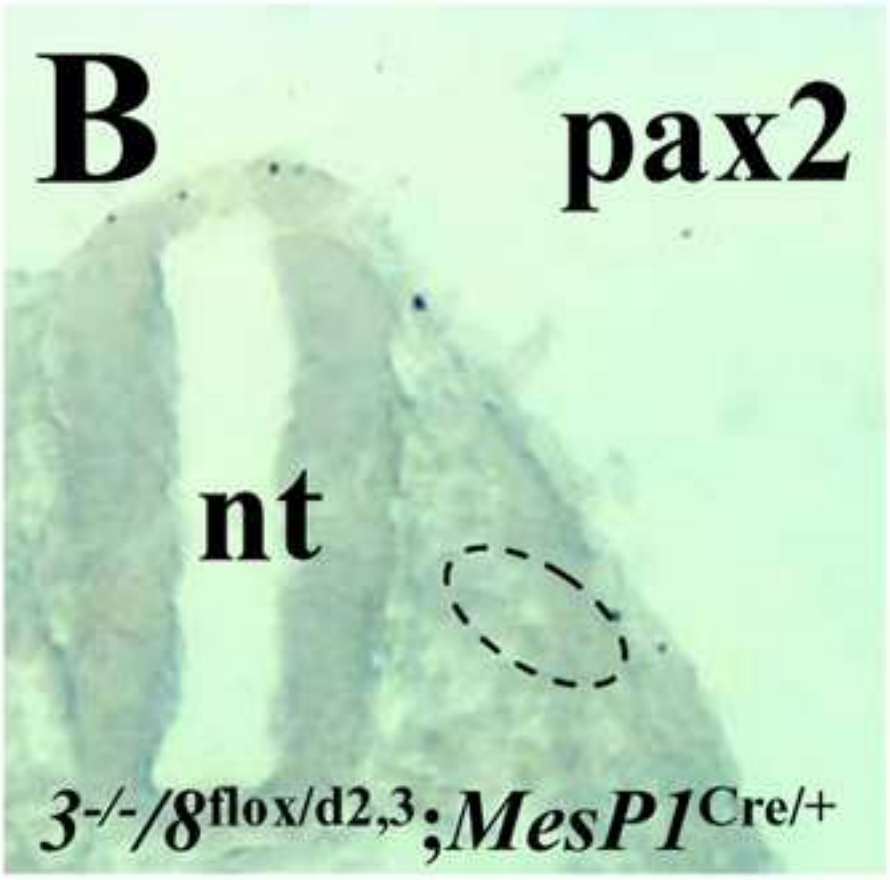

Supplementary Figure 3

Click here to download high resolution image

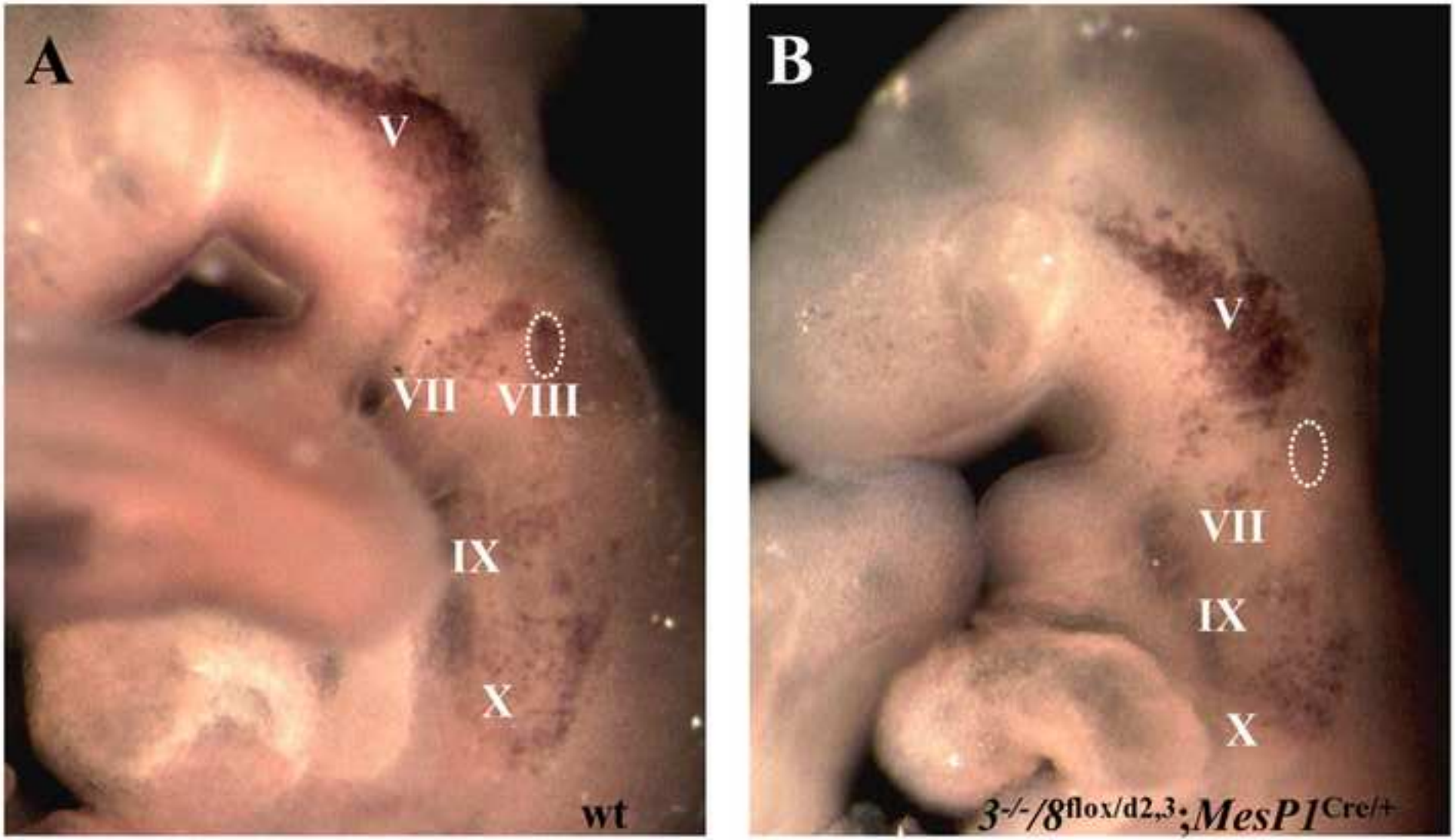

Supplementary Figure 4

Click here to download high resolution image

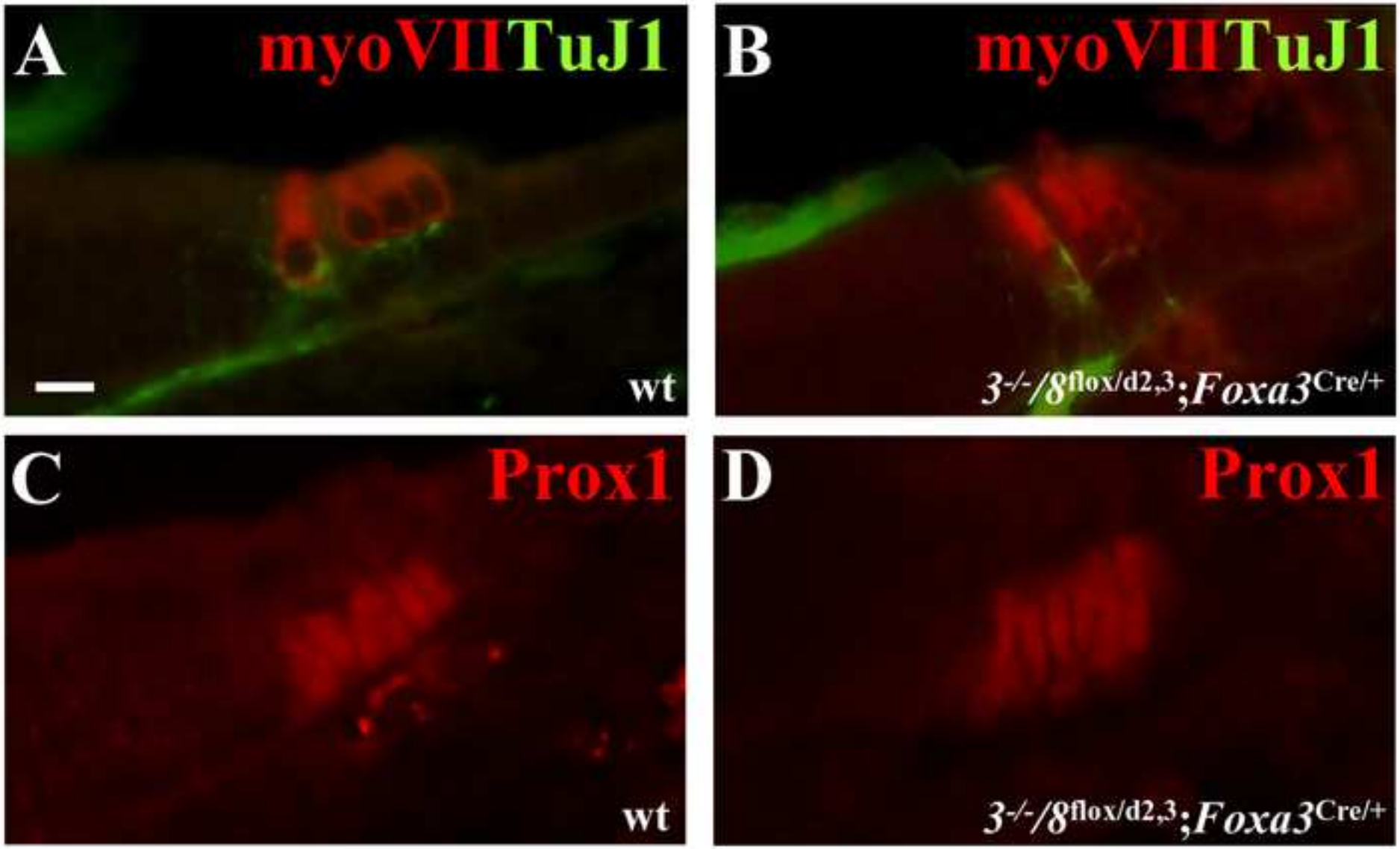

Supplementary Figure 5

Click here to download high resolution image

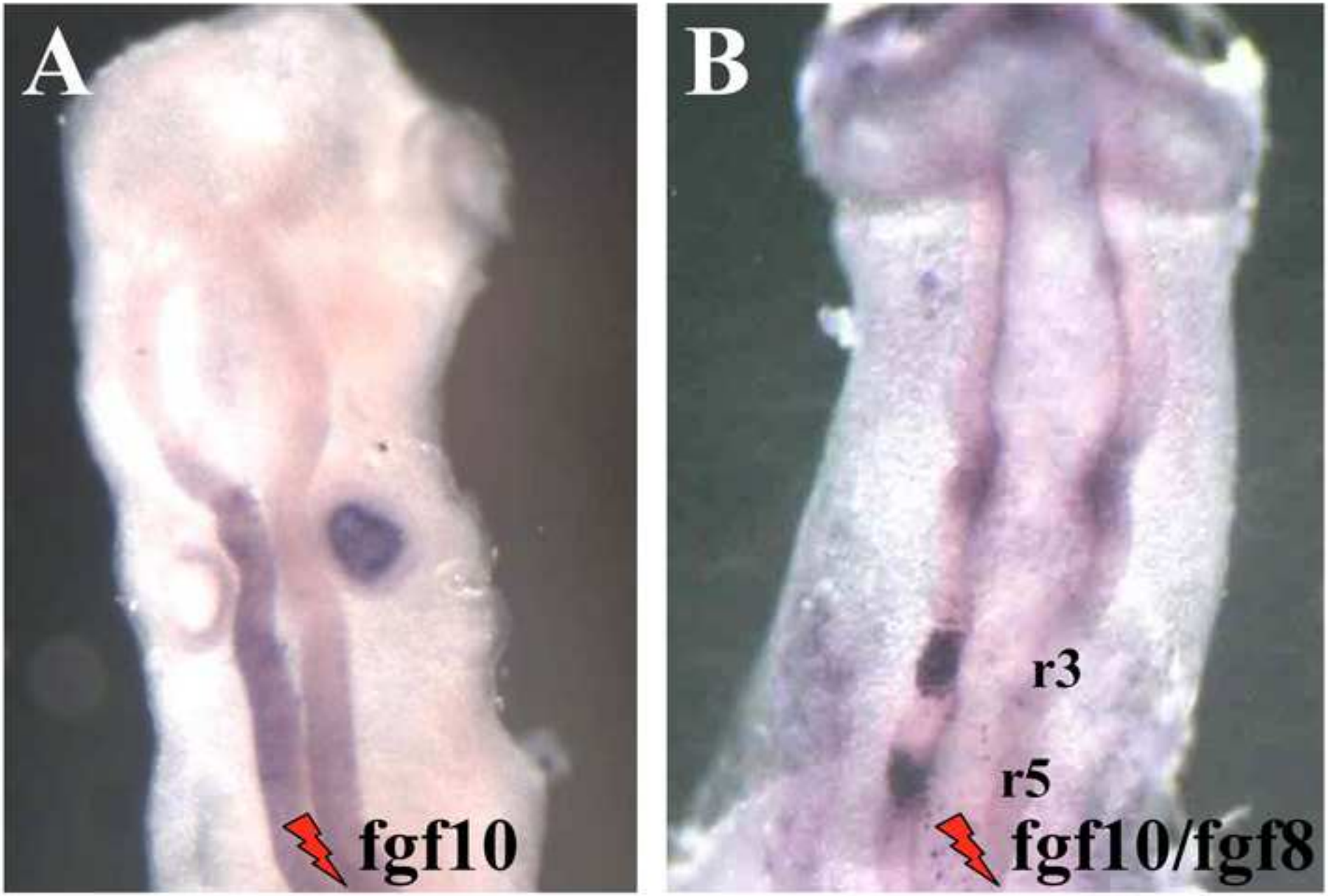

Supplementary Figure 6

Click here to download high resolution image

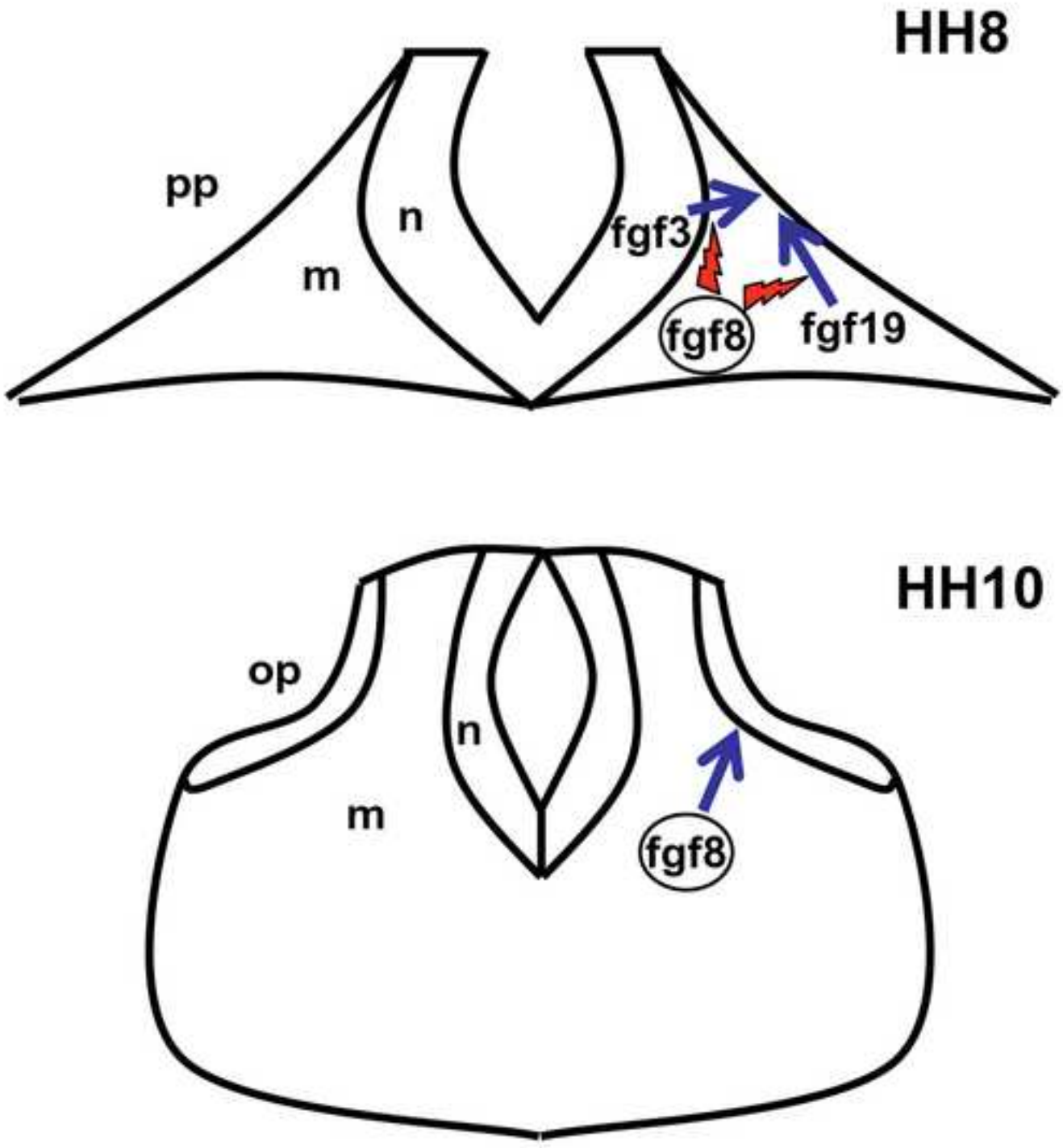

Supplementary Figure 7

Click here to download high resolution image